

PAPER • OPEN ACCESS

Feature Extraction based on Empirical Mode Decomposition for Shapes Recognition of Buried Objects by Ground Penetrating Radar

To cite this article: Hasimah Ali *et al* 2021 *J. Phys.: Conf. Ser.* **1878** 012022

View the [article online](#) for updates and enhancements.

You may also like

- [Estimation of Stellar Ages and Masses Using Gaussian Process Regression](#)
Yude Bu, Yerra Bharat Kumar, Jianhang Xie *et al.*
- [Analysis of dose distribution reproducibility based on a fluence map of in vivo transit dose using an electronic portal imaging device](#)
Didin Tardi, Aninda Fitriandini, Annisa Rahma Fauziah *et al.*
- [A new combined wavelet methodology: implementation to GPR and ERT data obtained in the Montagnole experiment](#)
L Alperovich, L Eppelbaum, V Zheludev *et al.*



ECS The Electrochemical Society
Advancing solid state & electrochemical science & technology

ECS UNITED

247th ECS Meeting
Montréal, Canada
May 18-22, 2025
Palais des Congrès de Montréal

Showcase your science!

Abstracts due December 6th

Feature Extraction based on Empirical Mode Decomposition for Shapes Recognition of Buried Objects by Ground Penetrating Radar

Hasimah Ali*¹, Mohd Shuhanaz Zonar Azalan¹, Ahmad Firdaus Ahmad Zaidi¹, Tengku Sarah Tengku Amran², Mohamad Ridzuan Ahmad², Mohamed Elshaikh³

¹School of Mechatronic Engineering, UniMAP, Arau, Perlis, Malaysia

²Nuclear Agency Malaysia, Bangi, Selangor,

³School of Computer and Communication Engineering, UniMAP, Pauh
hasimahali@unimap.edu.my

Abstract. Ground penetrating radar (GPR) is one of the promising non-destructive imaging tools investigations for shallow subsurface exploration such as locating and mapping the buried utilities. In practical applications, GPR images could be noisy due to the system noise, the heterogeneity of the medium, and mutual wave interactions thus, it is a complex task to recognizing the hyperbolic signature of buried objects from GPR images. Therefore, this paper aims to develop nonlinear feature extraction technique of using Empirical Mode Decomposition (EMD) in recognizing the four geometrical shapes (cubic, cylindrical, disc and spherical) from GPR images. A pre-processing step of isolating hyperbolic signature from different background was first employed by mean of Region of Interest (ROI). The hyperbolic signature that describes the shapes was extracted using EMD decomposition to obtain a set of significant features. In this framework, the hyperbolic pattern was decomposed of using EMD, to produce a small set of intrinsic mode functions (IMF) via sifting process. The IMF properties of the signature that exhibit the unique pattern was used as potential features to differentiate the geometrical shapes of buried objects. The extracted IMF features were then fed into machine learning classifier namely Support Vector Machines. To evaluate the effectiveness of the proposed method, a set data collection of GPR-images has been acquired. The experimental results show that the recognition rate of using IMF features was achieved 99.12% accuracy in recognizing the shapes of buried objects whose shows the promising result.

1. Introduction

Ground penetrating radar (GPR) is a promising technology utilized non-destructive test for shallow subsurface investigation such as land mines detection, mapping and locating buried utilities and archaeological works. Featuring fast response while keeping ground intrusion at minimal, GPR technology has sizeable impact in recent years, in which the applications of GPR not only limited to inspection of roads and bridges structures but it is widely used in concrete scanning, forensic investigation, mining and quarrying, geotechnical exploration, military, agriculture and forestry [1]. GPR uses high frequency electromagnetic (EM) wave propagation. The antenna module consist of transmitter and receiver is motioned along the ground surface, transmitting the waves into the ground.

Underground object as well as boundary interface possess contrasting dielectrics, causing partial reflection of waves that was transmitted on them. The receiving antenna then picks up the reflection signal [2]. Figure 1 shows basic GPR data imaging. In the acquisition phase, EM waves are transmitted and reflection signal are picked up by receiver, where reflection signals at specific depth form A-scan respective to each scanning points. When each scanning points of A-scan is compiled along a scanning path, B-scan pattern is formed, where as image, the signal are seen as hyperbolic pattern.

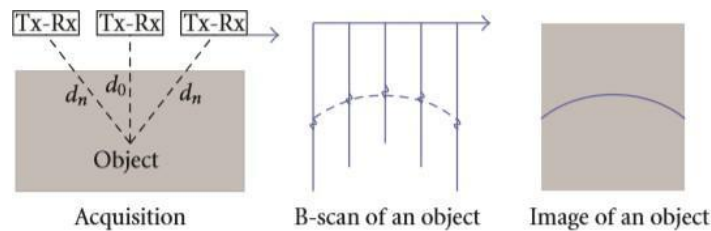


Figure 1: Basic imaging process of GPR data [3].

In the literature, many studies have been conducted to analyse the hyperbolic pattern for the purpose of detection and localization of the buried objects. Among the techniques used were histogram of oriented gradient (HOG) [4, 5], template matching [6, 7], neural network [8, 9, 10], genetic algorithm [11], Hough transform [12, 13], amplitude modulated signal [14], scale invariant feature transform [15]. For instance, Sagnard and Tarel [6] have conducted a study using GPR for detecting buried long sample pipes and able to extract features such as location, depth and lateral dimensions. Semi-automatic template-matching algorithm were developed by applying four main steps. Firstly, they defined the template using finite-difference time-domain simulations. Then, the raw GPR images were pre-processed in order to correct the variation and apply the template matching algorithm between hyperbola pattern of noisy environment with local zones to obtain a map of distances. Besides, min or max discrete amplitude were extracted through semi-automatic for each zone and lastly, they used non-linear least square as hyperbola model fitting to the discrete hyperbola data of GPR images.

Simi et al. [13] utilized Hough transform in hyperbola automatic detection algorithm (HADA) to detect the presence of the buried objects. In their work, the input GPR images were firstly pre-processed to remove background noise before subjected to feature extraction. In feature extraction, they used gradient filter with threshold to select stationary points that having the same phase polarity and phase detection. The linking procedure was then applied to assemble the edge pixels into connected sets. Then randomized Hough transform was utilized on labeled set to search the hyperbolic patterns and their apexes position in GPR images. The apexes position was related to the level of hyperbolic confidence by means of hyperbolic eccentricity which might reveal the depth and the propagation velocity of the EM in the soil. Even though Hough transform is wide-used in hyperbolic signature detection, this method is computationally costly due to the high resolution of GPR images and tendency to produce random output in noisy environment [16, 17].

Ni et al. [3] utilized multi-resolution technique using discrete wavelet transform for buried pipe detection as filtering method to enhance the GPR images for better quality profile images. They conducted the experiments using six different pipes model that consist of metal and non-metal materials with different scenarios of depth and locations. They found that the DWT profile produced more information compared to the traditional GPR profile. Further, Lu et al. [18] proposed two stage feature extraction technique of A-scan GPR data in to classify material of underground object. In first stage, they utilized the Discrete Wavelet Transform (DWT) of one-dimensional signal (A-scan) of GPR data where the approximation coefficient features of DWT sub-band were extracted. At second stage, the fractional Fourier Transform was used to transform the approximation coefficients into fractional domain and create fractional envelope curve to form feature vector before fed as input to the Support Vector Machines (SVM). The results show that their proposed features based SVM achieved good performance than statistical based frequency.

On the other hand, Kobashigawa et al. [8] investigated the capability of genetic programming over neural network in classifying the unexploded ordnance and non-unexploded ordnance objects of buried objects in GPR images. They simulated 2-D scattering patterns from one UXO target and four non-UXO object at various noise level and also using various cases of untrained data. Their results have shown that the genetic programming performed better than neural network.

Harkat et al. [11] have used Multi-Objective Genetic Algorithm (MOGA) to design a Radial basis function neural network classifier for GPR target detection. High order statistic cumulants of target samples were extracted as features on hyperbolas region of interest in GPR images. Then, the MOGA technique was used as features selection and mutual information derived from high order statistic cumulants to reduce the complexity of the problems.

Classification of GPR often requires dealing with complex qualitative features, scattering images and is carried out subjectively by human labours. This leads, inconsistency and subjective classification performance with respect to human factor are clearly inevitable [8]. Further, interpreting the GPR data especially hyperbolic signature is considered as challenging since an experienced human operator is required to analyse the complexity of GPR raw data. The problems were further hampered when the reflected signals underground objects are corrupted with noisy environments. Hence, these problems lead to the development of automated buried object detection and identification techniques based on GPR data.

Therefore, this research aims to classify the geometrical shapes of buried objects by incorporating a multiresolution technique called EMD as feature extraction in GPR images and Support Vector Machines (SVM) as a classifier. The justification for an initial focus on EMD features is motivated by the affinity of several aspects of EMD features to pre-existing feature extraction technique, making them suitable for utilities detection in GPR. Essentially, the EMD [18] is based on direct extraction of the signal energy associated with various intrinsic time scales. It is locally adaptive and well suited for analysis of nonlinear or non-stationary process. The EMD aims to consider oscillating signals at the level of their local oscillations. Any complex signal can be decomposed by EMD into a finite and in many cases small number of intrinsic mode functions (IMFs). In addition, EMD provides a decomposition technique to locally analyse the signal and separate the IMF component carrying the highest local frequency. Thus, in this research, the use of EMD technique to extract the IMF components as features from GPR images is investigated for classification process. The EMD offers fully data-driven solution, an alternative to using any-pre-determine filter, wavelet or Fourier-wavelet bases, leading to reduced feature extraction time.

Among the commonly used classifiers, SVM classifier also commonly used in various other fields of research, prominent for its efficiency and robustness [25]. The main principle of SVM is to find, in the input space the hyperplane that best distinguish two sets of training vectors. New vectors were then classified according to their position in comparison to the decision hyperplane. Consequently, the type of feature vectors used have strong impact on the degree of success for classification.

The paper is organized as follows. Section 2 discusses the materials and methodology used in the proposed methods. It consists of data collection and image pre-processing, feature extraction and classification. Section 3 contains the experimental results using the extracted EMD features of buried objects. Section 4 concludes the finding of the study.

2. Materials and Methods

The framework in Figure 2 shows the proposed method in classifying four shapes (cubic, cylindrical, spherical and disc) of metal buried object of hyperbolic pattern in GPR images. The working principle of each block is explained as follow:

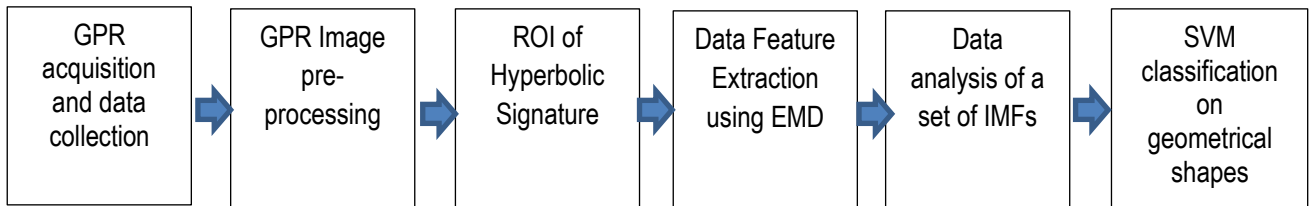


Figure 2: Framework of the proposed method

2.1. Data acquisitions of GPR images

In this experiment, we used the sandbox test bed having the dimension of 2.5 m long, 1.5 width, 1.5 m setup by Agency Nuclear Malaysia (ANM) [20]. The test bed was made entirely of wood, to avoid metal material that might cause interference to GPR operation and signals fidelity. Six (6) tons of dry sand has been used in this experiment as the medium [20]. This soil medium was selected as it represents the ‘best’ condition to observe the presence of buried objects. Figure 3 shows the sandbox test bed and soil medium used in the experiment.



Figure 3: Sandbox test bed (left) and soil medium (right).

GPR system unit. Figure 4 shows the GPR system unit. It consists of a few components which are antenna transmitter and receiver, battery, control unit, and vision ground software. The RAMAC/GPR 800 MHz shielded antenna has been used for the GPR scanning as well as for the data collection. In this experiment, four geometrical shapes such as cubic, cylindrical, spherical and disc were employed as samples of buried targets. These samples were then buried in the sandbox test bed with depth of 20 cm from the top surface individually. Figure 5 shows the samples of buried objects and position of the samples buried in the testbed.



Figure 4. GPR system



Figure 5. Example of samples used in the experiment (left) and sample buried in the testbed (right).

The samples were made up aluminum. The mapping and scanning operation of GPR system were supervised by the authorized officer of Non-Destructive Test-Material Structure Integrity Group at ANM.

In total, 340 digitized GPR images were acquired made of 87 cubic images, 82 cylindrical images, 86 disc and 85 spherical images using RAMAC MALA GPR system with antenna frequency of 800 MHz.

2.2. GPR image pre-processing

Pre-processing is essential and have high impact on overall performance of the recognition system. First, the raw image was scaled and cropped based on region of interest (ROI) of hyperbolic pattern into a fixed, standard size. Figure 6 shows the original binary images and the pre-processed GPR images. The pre-processed images were then subjected to the empirical mode decomposition (EMD) for extracting the GPR features based on hyperbolic signature.

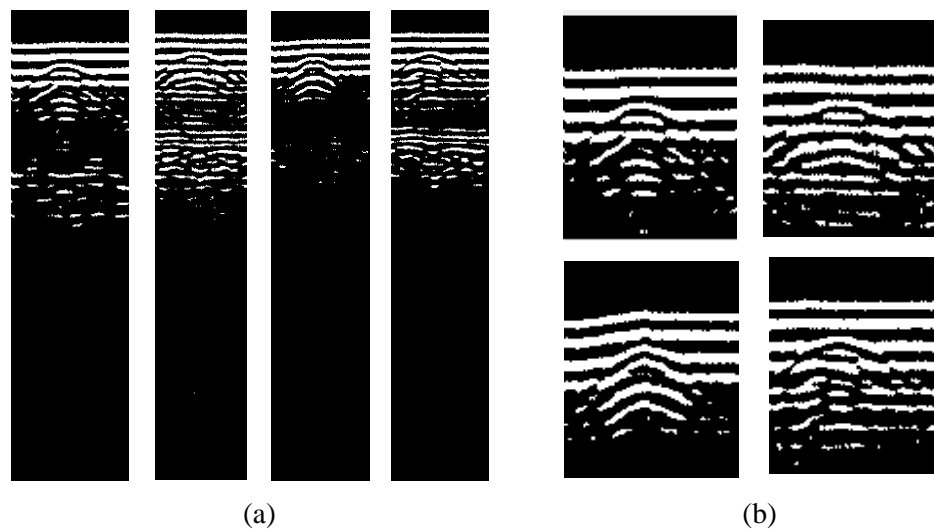


Figure 6. (a) original images of GPR images in binary form starting with cubic, cylindrical, disc and spherical (left to right), (b) region of interest of hyperbolic signature images of cubic, cylindrical (top) and disc, sphere (bottom)

2.3. Empirical Mode Decomposition for Feature Extraction

Empirical mode decomposition is a multiresolution technique proposed by Huang et al. [18] used to decomposed any complicated signal and suitable for non-linear and nonstationary data analysis as sum of zero-mean AM and FM components. The main advantages of EMD is that it approach is fully data-driven and always exhibit high decomposition efficiency and sharp localization in term of frequency and also time. It is locally adaptive and multiscale. Initial study of EMD was focus on the ocean waves signal, and then found potentially in the field of biomedical applications [21, 22], face analysis [23, 24] and etc. In different aspect, the EMD seeks to reveal the characteristic about local trends in the signal by investigating the signal oscillations. These oscillation can be quantizing by local details or local trends. The basic concepts of EMD lie on the utilization of the interpolation technique such as cubic spline, sifting process to extract the intrinsic mode function and numerical convergence criteria to stop the sifting process. The EMD algorithm essentially, decompose the signal in which two criteria must be satisfied in order to extract a number of the intrinsic mode functions (IMFs) : (1) the number of extrema and the number of zero crossings are either equal or differ at most by one; and (2) at any point, the mean of its upper and lower envelopes equal zero. The above two conditions fulfil the necessary condition to define a significant instantaneous frequency. The basic principle of EMD algorithm is as follows. Suppose given the signal $x(t)$,

1. Identify all the extremas (local maxima and local minima) of $x(t)$. Then, Let $s(t) = x(t)$.
2. Interpolate all the extremas (local maxima and the local minimum) to create upper envelope $e_u(t)$ and lower envelope $e_l(t)$, respectively using cubic spline interpolation.
3. Compute the mean envelope by $m(t)$: $m(t) = [e_{upper}(t) + e_{lower}(t)]/2$.
4. Sifting: $d(t) = s(t) - m(t)$ (via sifting process).
5. Check the two condition of $d(t)$:
If $d(t)$ is not an IMF, then let $d(t)=s(t)$ and repeat to item (1). If $d(t)$ is an IMF, then let $c_1(t)=d(t)$ and end the process.

The residue signal $r(t) = x(t) - c_1(t)$ is considered as new signal [i.e. $s(t)=r_1(t)$] and same iteration is conducted to the new signal to extract next IMF and producing the subsequent residue. Such process is proceed until the sifting process is stopped by any of the mentioned criteria. Once extracting n numbers of IMFs, $r_n(t)$ becomes either an IMF or monotone trend which known as the dc component of the signal. As EMD possesses the advantages of signal reconstruction, the equation of:

$$x(t) = \sum_{i=1}^n c_i(t) + r_n(t) \quad (1)$$

can be used to obtain the original signal

2.4. Support Vector Machines Classification

SVM is one of popular machine learning technique and gaining popularity due to good generalization performance. It based on the structural risk minimization that exhibit superior than empirical risk minimization (conventional NN). SRM focus on minimizing an upper boundary of expected risk, in contrast the ERM minimizing the training error [25]. SVM has been widely used for classification and also regression of data analysis. The objective of SVM is to seek the 'optimal' hyperplane by means of the margin is maximized (the data points have the largest distance from the hyperplane). Based on the applications, SVM can be adopted as linear separable and nonlinear separable case. To illustrate the separable case, lets considered a set of supervised training data with class label denoted as $\{(x_1, y_1), (x_2, y_2), \dots, (x_k, y_k)\}$ in which $i = 1, 2, \dots, k$ for $x \in R^n$ and $y \in \{1, -1\}^k$. Lets class 1 ($y = 1$) and class 2 ($y = -1$) are separated by the hyperplane having equation of:

$$(w \cdot x) + b = 0 \quad (2)$$

in compact form the equation becomes:

$$y_i[(w \cdot x_i) + b] \geq 1, \quad i = 1, 2, \dots, k \quad (3)$$

Figure 7 depicts the SVM for linear separable case.

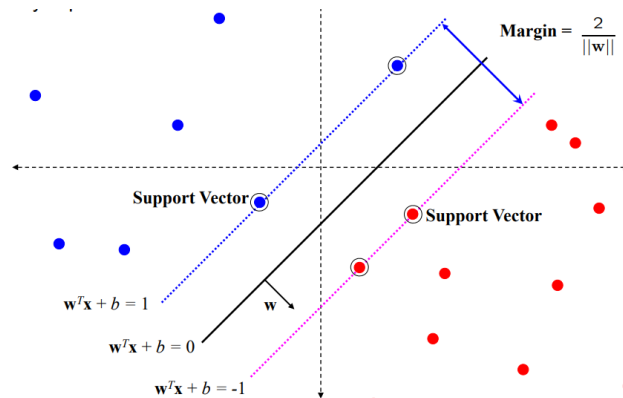


Figure 7. SVM with linear separable

The data that lie on the margin we called the support vectors. Whereas, the margin is defined by eqn. (4) as the distance from hyperplane to the closest data points:

$$d_1 + d_2 = \frac{2}{\|w\|} \quad (4)$$

The hyperplane of the two classes is said 'optimal' when the margin (distance from hyperplane) is maximized. Thus, minimizing the eqn. (5) results in optimal separation of hyperplane:

$$\Phi(w) = \frac{1}{2} \|w\|^2 \quad (5)$$

For nonlinear-case, slack variable is adopted, which to minimize:

$$\frac{1}{2} \|w\|^2 + C \left(\sum_i L(\xi_i) \right) \quad (6)$$

The C and L are the adjustable penalty term and loss function (linear case), respectively. The use of Lagrangian method with linear loss in optimization of eqn. (2) is to maximize:

$$L_D(w, b, \alpha) = \sum_i \alpha_i - \frac{1}{2} \sum_{i=1}^k \sum_{j=1}^k \alpha_i \alpha_j y_i y_j x_i^T x_j \quad (7)$$

Where,

$$0 < \alpha_i \leq C, \quad i = 1, 2, \dots, k \quad (8)$$

and

$$\sum_i \alpha_i y_i = 0 \quad (9)$$

Noted that, α_i is a set of the Lagrangian multiplier. Optimization can done using quadratic programming and the optimized parameters are:

$$w = \sum_i \alpha_i y_i x_i \quad (10)$$

Note also $\alpha_i = 0$, for every x_i except the ones located on the margin. Thus training data with $\alpha_i \neq 0$ are termed as support vectors. For nonlinear data problem, a kernel function is introduced. It used to map

kernel function from low dimensional feature space into higher dimensional space to be linearly separable. General choice of kernel functions includes linear, polynomial, radial basis function and sigmoid functions. In this experiment, radial basis function or radial kernel was adopted to map the IMF features into higher dimensional IMF features space. The results will be presented in the subsequent section.

3. Results and Discussions

3.1. Applied EMD on GPR images

In this experiment, EMD algorithm based on Huang et al [18] has been used to extract a small set of intrinsic mode functions (IMFs) on GPR images via sifting process. The GPR images have been decomposed using EMD technique to produce a set of intrinsic mode functions (IMFs) which is IMF 1, IMF 2, IMF 3 and a residue.

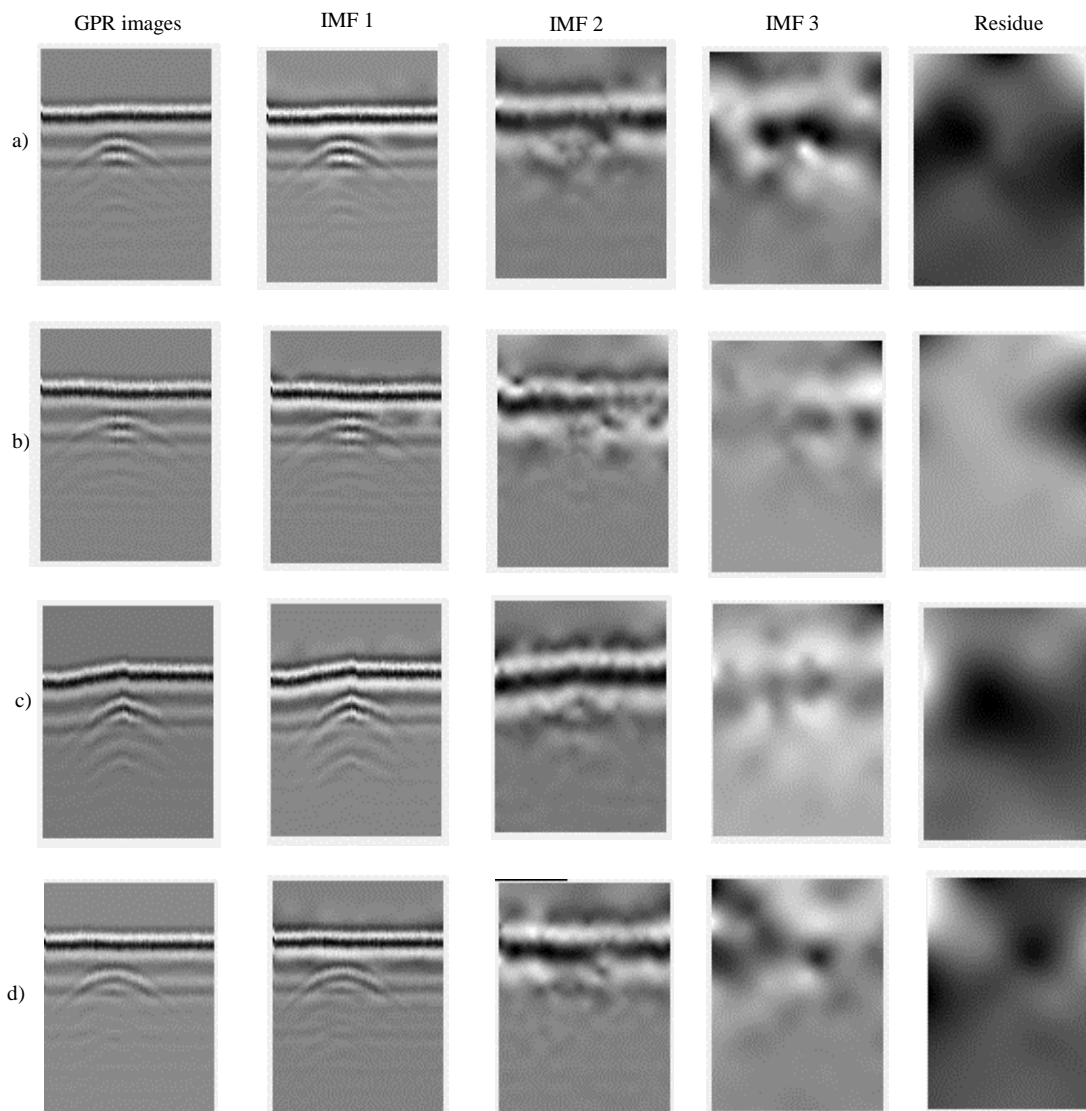


Figure 8. The GPR images and their corresponding IMFs (IMF 1, IMF 2, IMF 3) and residue using EMD algorithm for geometrical shape: a) cubic, b) cylindrical, c) disc and d) spherical

Figure 8 shows the results of EMD decomposition on GPR images in terms of IMF 1, IMF 2, IMF 3 and residue for cubic, cylindrical, disc and spherical shapes. Based on the Figure 8, it can be inferred that the IMFs reveal the pattern structure from the finest to coarsest of the original image. The relative mean of the data decays to zero when the order of the IMF increases, reflecting the nature of EMD. In other words, the lower order of IMF exhibits fast oscillation mode while the higher order of IMF exhibits slow oscillation modes and the monotonic or constant trend exhibit the residue. The first IMF (IMF1) effectively contains the largest magnitude extrema in the GPR images which contribute to the highest local information that describe the characteristic of distinct geometrical shape of GPR images

3.2 Experimental Results and Discussion

To evaluate the proposed method, 340 images were acquired consisting of 87 cube, 82 cylinder, 86 disc and 85 sphere. Firstly, the GPR images were pre-processed by utilizing, background removal, cropping to obtained uniformity of the images. Then, the GPR images were decomposed into a set of intrinsic mode functions (IMFs) which is IMF1, IMF2, IMF3 and residue using empirical mode decomposition via sifting process. The IMF features then were subjected as input to SVM classifier for recognition process. Table 1 presents the mean and standard deviation of different IMFs for different shapes of buried objects.

Table 1: The mean and standard deviation of EMD features (IMF1, 2, 3 and residue) of geometrical shapes (cubic, cylindrical, disc and spherical).

	IMF 1	IMF 2	IMF 3	RESIDUE
Cubic	0.5246 ± 0.0505	0.5134 ± 0.356	0.5086 ± 0.0356	0.4438 ± 0.0320
Cylindrical	0.5340 ± 0.0291	0.5137 ± 0.0374	0.5145 ± 0.0332	0.4741 ± 0.0273
Disc	0.5307 ± 0.0758	0.5130 ± 0.0532	0.5096 ± 0.0348	0.4414 ± 0.0255
Sphere	0.5310 ± 0.0262	0.5162 ± 0.0336	0.5189 ± 0.0336	0.4381 ± 0.0293

In this experiment, 10-fold cross-validation was used. The whole dataset (340 images) is randomly divided into ten sets of having the same distribution of different GPR images. At each time of the process, nine sets (306 images) used for training the classifiers and the remaining set (34 images) used for testing. The process was repeated for 10 times using different set and final average was calculated.

3.2.1 Classification using IMF1 features + SVM classifiers

Table 2 presents the confusion matrix of the first intrinsic mode function (1st IMF features) using SVM classifier in classifying four geometrical shapes. As observed in Table 2, the disc shape provides the highest recognition rate at 97.67 %, whereas cylindrical shape contributes the lowest rate at 68.29 %. On the other hand, spherical and cubic shapes show the recognition rates of 94.12 % and 83.91 %, respectively. Based on the results obtained, twenty-one (21) out of 86 cylindrical shape are misclassified with disc shape. This shows that the first IMF of cylindrical features may be resemble to the first IMF of disc features. This resemblance may occur due to inter-class similarity of hyperbolic features either in cylindrical or disc shape thus results in low accuracy. We then further investigate the second IMF features using SVM classifier.

Table 2: Confusion matrix of first IMF features using SVM classifier for cubic, cylindrical, disc and spherical shapes.

	Cubic	Cylindrical	Disc	Sphere	<i>Average</i>
Cubic	73	1	0	0	
Cylindrical	5	59	0	1	
Disc	9	21	84	4	
Sphere	0	1	2	80	87.06%
<i>Total</i>	87	82	86	85	340

3.2.2 Classification using IMF2 features + SVM classifiers.

Table 3 shows that the confusion matrix of second IMF using SVM classifier for above mentioned geometrical shapes. It can be seen from Table 3 that; the spherical shape contributes the highest recognition rate which is 100% accuracy. On the other hand, cubic, cylindrical and disc shapes have shown promising results with approximately 98 % accuracy. It observed that one (1) out of 87 cubic shape is misclassified with disc shape, one (1) out of 82 cylindrical shape is misclassified with cubic shape and one (1) out of 86-disc shape is misclassified with cylindrical shape. It shows that the IMF2 features may contains significant information that able to classify the geometrical shapes of cubic, cylindrical, disc and spherical.

Table 3: Confusion matrix of IMF2 features using SVM classifier for cubic, cylindrical, disc and spherical shapes.

	Cubic	Cylindrical	Disc	Sphere	<i>Average</i>
Cubic	86	1	0	0	
Cylindrical	0	81	1	0	
Disc	1	0	85	0	
Sphere	0	0	0	85	99.12%
<i>Total</i>	87	82	86	85	340

As overall, the average recognition rate of IMF2 features using SVM classifier provides better results compared to the IMF1 features using SVM. The performance of the proposed method is also compared with previous work. Table 4 shows the summary of the existing work of the GPR based on hyperbolic pattern. It has been reported that in many studies in the literatures have used different approaches to analyse and interpret the hyperbolic pattern in exacting various information that related to subspace exploration.

While direct performance comparison between different techniques may not be viable due to variability of applications, experimental setup, type of materials, number of features used as well as different approach adopted in dataset partitioning, distinctive results of every approach can still be achieved. It is telling from Table 4 that, the proposed method of using empirical mode decomposition with SVM classifier for shape recognition in GPR images has achieved 99.12% accuracy, thus shows a promising result.

Table 4: Comparison the proposed method with previous work

Authors	Application	Methods	Classifier	Accuracy
Lu et al.[18]	Material classification	DWT+ Fractional Fourier Transform	SVM	95 % (9training sample)
Harkat et al. [11]	Target and non-target samples	High order statistic cumulant	Multi-objective Genetic Algorithm	97.87 with 80 features
Ni et al. [2]	Buried pipe detection	DWT used for reconstruction GPR profiles	-	Error < 10 % in estimating location and depth.
Lee & Mokji. [5]	Target detection	HOG	Linear SVM	93.75%
Proposed method	Shape recognition	EMD	SVM	99.12%

4. Conclusions

This paper has presented the used of empirical mode decomposition technique as feature extraction with SVM classifier in recognizing four geometrical shape such as cube, cylindrical, disc and sphere based on hyperbolic pattern in GPR images. In this framework, a set of intrinsic mode function was obtained by EMD via sifting process namely IMF1, IMF2, IMF3 and residue. The IMF pattern structure reveals from finest to coarsest of the original image. This is due to the nature of EMD, as the lower order of IMF exhibits fast oscillation mode while the higher order of IMF exhibits slow oscillation modes. The extracted IMF2 was used for shape recognition. Based on the results obtained, the highest recognition rate using IMF2 features with SVM classifier has achieved 99.12% in recognizing four geometrical shapes. Thus, the used EMD as feature extraction in recognizing shape based on hyperbolic signature in GPR images is promising. In future, further study should conducted using EMD in recognizing shape of unknown target.

Acknowledgement

This project has been supported by Nuclear Agency Malaysia by providing GPR RAMAC/MALA system under MoU agreement.

References

- [1] W W-L Lai, X Derobert, P Annan. A review of Ground Penetrating Radar application in civil engineering: A 30-year journey from locating and testing to imaging and diagnosis, NDT and E International, 96(2018) 58-78.
- [2] S. H. Ni, Yan Hong Huang, Kuo Feng Lo, Da Ci Lin. Buried pipe detection by ground penetrating radar using the discrete wavelet transform. 2010 Computers and Geotechnics. Vol(37). Issue 4. 440-448.
- [3] Syambas N R 2012 *An Approach for Predicting the Shape and Size of a Buried Basic Object on Surface Ground Penetrating Radar System*. Hindawi Publishing Corporation International Journal of Antennas and Propagation Volume 2012.
- [4] P. A. Torrione, K. D. Morton, R. Sakaguchi, L.M. Collins. Histograms of Oriented Gradients for Landmine Detection in Ground-Penetrating Radar Data, IEEE Transactions on Geoscience and Remote Sensing, Vol. 52, No.3 (2014), 1539-1550.
- [5] Lee K L, Mokji M M 2014 *Automatic Target Detection in GPR Images Using Histogram of*

- Oriented Gradients (HOG)*. 2nd International Conference on Electronic Design (ICED), August 19-21, Penang, Malaysia
- [6] F. Sagnard & J.P. Tarel. Template-matching based detection of hyperbolas in ground-penetrating radargrams for buried utilities. *Journal of Geophysics and Engineering*, 13(2016), 491-504
- [7] N. R. Syambas. An approach for predicting the shape and size of a buried basic object on surface ground penetrating radar system, *International Journal of Antennas and Propagation*, Vol 2012
- [8] J. S. Kobashigawa ; H.-S. Youn ; M. F. Iskander ; Z. Yun , Classification of Buried Targets Using Ground Penetrating Radar: Comparison Between Genetic Programming and Neural Networks. *IEEE Antennas and Wireless Propagation Letters* .Volume: 10. (2011) 971 – 974.
- [9] K. Ishitsuka, S. Iso, K. Onishi & T. Matsuoka. Object detection in Ground Penetrating Radar images using a Deep Convolutional Neural Network and Image Set Preparation by Migration, *International of Geophysica*, Vol 2018
- [10] X. L Travassos, S. L. Avila & N. Ida. Artificial Neural Networks and Machine Learning techniques applied to ground penetrating radar: A review, *Applied Computing and Informatics*, 2018.
- [11] H. Harkat, A. Ruano, M. G. Ruano & S. D. Bennani. Classifier design by a multi-objective genetic algorithm approach for GPR automatic target detection, *IFAC PapersOnLine* 51-10(2018) 187-192
- [12] M. J. Carlotto, Detecting Buried Mines in Ground Penetrating Radar using a Hough Transform Approach, *Proceeding Volume 4741, Battlespace Digitization and Network-centric WarfareII*, 2002
- [13] A. Simi, S Bracciali & G. Manacorda. Hough transform based automatic pipe detection for array GPR: Algorithm Development and on-site tests, 2008 IEEE Radar Conference.
- [14] L. Qao, Y. Qin, X. Ren & Q. Wang. Identification of Buried objects in GPR using amplitude modulated signals extracted from multiresolution monogenic signal analysis, *Sensors (Basel)*, Vol. 15(12), 2015 Dec, 30340-30350.
- [15] H. Harkat, Y. Elfakir, S. D. Bennani, G. Khaissidi & M. Mrabi. Ground Penetrating Radar Hyperbola Detection Using Scale Invariant Feature Transform, 2nd International Conference on Electrical and Information Technologies ICEIT 2016.
- [16] Q. Dou, L. Wei, D. R. Magee & A. G. Cohn. Real Time Hyperbolae Recognition And Fitting In GPR Data, *IEEE Transactions on Geoscience and Remote Sensing*, 55 (1), 2017, pp. 51-62.
- [17] H. Harkat, A. Ruano, M. G. Ruano & S. D. Bennani. Classifier Design By A Multi-Objective Genetic Algorithm Approach For Gpr Automatic Target Detection, *IFAC PapersOnLine* 51-10(2018) 187-192.
- [18] Q. Lu, J. Pu, and Z. Liu. Feature Extraction and Automatic Material Classification of Underground Objects from Ground Penetrating Radar Data, *Journal of Electrical and Computer Engineering*, Volume 2014, Article ID 347307.
- [19] Norden E. Huang, Zheng Shen, Steven R. Long , Manli C. Wu , Hsing H. Shih, Quanan Zheng , Nai-Chyuan Yen , Chi Chao Tung and Henry H. Liu. The empirical mode decomposition and the Hilbert spectrum for nonlinear and non-stationary time series analysis, *Proceeding of The Royale Society. Mathematical, Physical and Engineering Sciences*, 1998.
- [20] T. S. T. Amran, M. P. Ismail, M. R. Ahmad, M. S. M. Amin, M. A. Ismail, S. Sani, N. A. Masenwat & N. S. M. Basri. Monitoring Underground Water Leakage Pattern By Ground Penetrating Radar Using 800 Mhz Antenna Frequency. *IOP Conf. Series: Material Science and Engineering* 298 (2018).
- [21] A. Gallix, J.M. Gorriz, J. Ramirez, I.A. Illan, E. W Lang. On the empirical mode decomposition applied to the analysis of brain SPECT images, *Expert Systems with Applications*, 39 (2012), 13451-13461.
- [22] R. B. Panchori. Discrimination between Ictal and Seizure-Free EEG Signals using Empirical Mode decomposition, *Research Letter in Signal Processing*, Vol 2008
- [23] R. Bhagavatula & M. Savvides. Analyzing facial images using empirical mode decomposition for illumination artifact removal and improved face recognition, 2007 IEEE International Conference on Acoustics, Speech and Signal Processing, 2007

- [24] H. Ali, M. Hariharan, S. Yaacob, A. H. Adom. Facial emotion recognition using empirical mode decomposition. *Expert Systems With Applications, Volume 42, Issue 3, 15 February 2015, pp 1261-1277*
- [25] S. R. Gunn. Support Vector Machines for Classification and Regression. Technical Report, 1988